Proceedings of ICFDP8:
8th Int. Congress of Fluid Dynamics & Propulsion
December 14-17,2006,Sharm El Shiekh, Sinai, Egypt.

ICFDP8-EG-142

A DETAILED COMPUTATIONAL ANALYSIS OF THE FLOW OVER A HIGH SPEED TRAIN FITTED WITH GUIDE VANES

I. K. Mohamed
Higher Institute of Energy
South Valley University, Aswan, Egypt.

M.A.Serag-Eldin
Mechanical Engineering Department
American University in Cairo, Cairo, Egypt.

A.S.Sabry
Mechanical Engineering Department
Cairo University, Cairo, Egypt.

Y.P.Kohama
Institute of Fluid Science, Tohoku University, Sendai, Japan.

ABSTRACT

The present paper employs computational modeling to analyze the full three-dimensional flow over a high speed train in which longitudinal fins have been introduced in the front and rear in order to reduce trailing edge vortices.

Many of the intricate details of the flow are revealed. Moreover, an evaluation is made of the often neglected compressibility effects as well as the effects of the relative motion between train and ground.

The computational model adopted comprises the three-dimensional form of the mass conservation and momentum equations, and the transport equations for the RKE turbulence model; it was validated elsewhere against experimental measurements. An unstructured grid is used which fits the boundary geometry very closely and allows grid refinement in critical regions.

INTRODUCTION

High speed trains are currently gaining popularity in view of their economy relative to airplanes, and speed compared to other forms of land transportation. Recently train speeds have exceeded 300 km/hr. Thus aerodynamic drag is now the chief factor in determining train speed and performance, Kohama et al(1992). At 300 km/hr, a train can use up to 90% of the traction power available at the wheels to overcome aerodynamic drag, King et al (1993).

The aerodynamic drag force is dependent on the cross-sectional area of the train body, train length, shape of train fore and after-bodies, surface roughness of train body, and ground topography surrounding the traveling train, Raghu et al (2002). One of the most important design requirements for high speed trains is a highly aerodynamic frontal nose and rear end. Moreover, because most high speed trains run in both directions, the nose and rear end shapes are usually identical.

The present study deals with the aerodynamics of a high speed train in which directional fins have been added to the leading/trailing sections in order to control the generated trailing end vortices. The main objective of the paper is to analyze the resulting flow and demonstrate the high degree of streamlining that may be realized when carefully designed directional fins are employed.

The investigations are based on flow predictions made with the aid of a computational model which was validated elsewhere, Mohamed(2006). First, the geometry of the considered train is presented. The computational model is then described. The resulting predictions are subsequently displayed with the aid of velocity vectors and Mach number contour lines, and duly discussed. Finally a summary and conclusion is presented.

NOMENCLATURE

A_0 ,A_s	RKE turbulence model contants
E	total energy/unit mass
G_k	rate of generation of k
k	turbulence kinetic energy
M	Mach number
q	total heat flux
S_k,S_ε	k, ε source terms
u,v,w	components of V in x,y,z directions.
x,y,z	Cartesian coordinates directions
V	velocity vector
$\forall$	volume of cell
C_2,$C_{1\varepsilon}$	are turbulence model constants.

Greek letters

ε	rate of dissipation of k
ρ	fluid density
τ	viscous stress tensor
$\sigma_k,\sigma_\varepsilon$	are turbulent Prandtl numbers for k and

TRAIN GEOMETRY

The train geometry considered in the present investigation features identical nose and trailing end shapes, connected by a continuous straight tube of uniform cross-section, representing main train body. For economy of calculations, the adopted tube length is much shorter than that in a real train; however, the extra length is not expected to introduce new features in the investigated flow. This practice is also very common in experimental investigations.

Figure 1 reveals the train geometry that will be employed in the present investigations; the nose and rear ends are similar to the Japanese Shinkansen series 300. The dimensions are in millimeters and correspond to a scaled down model for which experimental measurements are available and have been employed to validate the mathematical model, Mohamed(2006). The train height is 110 m.m.

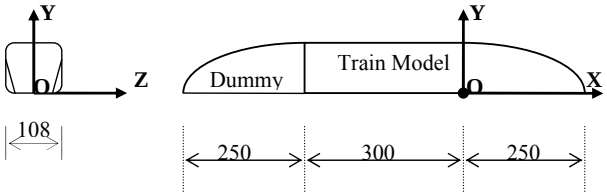

Figure 1. Train geometry employed for investigations.

Figure 2 shows a picture of the train model displaying clearly the longitudinal fins on either side of the train nose.

Figure 2. Picture of train model displaying longitudinal fins.

MATHEMATICAL MODEL

Governing Equations

The governing equations, cast in integral Cartesian coordinates for an arbitrary control volume $\forall$ with differential surface area dA, may all be cast in the following general form:

$$\frac{\partial}{\partial t}\int_{\forall} W\,d\forall + \oint [F - G].dA = \int_{\forall} H\,d\forall \qquad (1)$$

Where the vectors W, F and G are defined as the vectors:

$$W = \begin{Bmatrix} \rho \\ \rho u \\ \rho v \\ \rho w \\ \rho E \end{Bmatrix}, \quad F = \begin{Bmatrix} \rho V \\ \rho V u + p\hat{i} \\ \rho V v + p\hat{j} \\ \rho V w + p\hat{k} \\ \rho V E + pV \end{Bmatrix}, \quad G = \begin{Bmatrix} 0 \\ \tau_{xi} \\ \tau_{yi} \\ \tau_{zi} \\ \tau_{ij} v_j + q \end{Bmatrix} \qquad (2)$$

and the vector H contains source terms such as body forces and energy sources.

Here ρ, V, E, and p are the density, velocity vector, total energy per unit mass, and pressure of the fluid, respectively. τ is the viscous stress tensor, and q is the heat flux.

Turbulence Model

In order to render the computations tractable, the instantaneous time-dependent equations(1) are time averaged, and a turbulence model employing the effective viscosity concept is employed. This results in the disappearance of the time-derivative term, and the replacement of the viscous stresses with effective turbulence stresses.

The turbulence model adopted here is the Realizable k- ε model (RKE), Shish et al(1995). It was tested against corresponding measurements and found to give excellent agreement with measurements, Mohamed(2006); and also to yield best results among seven other models tested.

The modeled transport equations for k and ε in the realizable k-ε model are:

$$\frac{\partial}{\partial t}(\rho k)+\frac{\partial}{\partial x_i}(\rho k u_j)=\frac{\partial}{\partial x_i}\left(\left(\mu+\frac{\mu_t}{\sigma_k}\right)\frac{\partial k}{\partial x_j}\right)+G_k+G_b-\rho\varepsilon-Y_M \qquad (3)$$

and

$$\frac{\partial}{\partial t}(\rho\varepsilon)+\frac{\partial}{\partial x_j}(\rho\varepsilon u_j)=\frac{\partial}{\partial x_j}\left[\left(\mu+\frac{\mu_t}{\sigma_\varepsilon}\right)\frac{\partial\varepsilon}{\partial x_j}\right]-\rho C_2\frac{\varepsilon^2}{k+\sqrt{\nu\varepsilon}}+C_{1\varepsilon}\frac{\varepsilon}{k}C_{3\varepsilon}G_b \qquad (4)$$

In the above equations, G_k represents the generation of turbulence kinetic energy due to the mean velocity gradients; G_b is the generation of turbulence kinetic energy due to buoyancy; Y_M represents the contribution of the fluctuating dilatation in compressible turbulence to the overall dissipation rate. C_2 and $C_{1\varepsilon}$ are constants. σ_k and σ_ε are the turbulent Prandtl numbers for k and ε, respectively.

As in other k-ε models, the eddy viscosity is computed from

$$\mu_t = \rho C_\mu \frac{k^2}{\varepsilon} \tag{5}$$

with C_μ computed from:

$$C_\mu \equiv \frac{1}{A_0 + A_S \frac{kU^*}{\varepsilon}} \tag{6}$$

where

$$U^* \equiv \sqrt{S_{ij}S_{ij} + \tilde{\Omega}_{ij}\tilde{\Omega}_{ij}} \tag{7}$$

and

$$\tilde{\Omega}_{ij} = \Omega_{ij} - 2\varepsilon_{ijk}\omega_k \quad , \qquad \Omega_{ij} = \overline{\Omega_{ij}} - \varepsilon_{ijk}\omega_k \tag{8}$$

Where Ω_{ij} is the mean rate of rotation tensor viewed in a rotating reference frame with the angular velocity ω_k. The model constants A_0 and A_s are given by

$$A_0 = 4.04 \quad , \qquad A_S = \sqrt{6}\cos\phi \tag{9}$$

where

$$\phi = \frac{1}{3}\cos^{-1}\left(\sqrt{6}W\right), \quad W = \frac{S_{ij}S_{jk}S_{ki}}{\tilde{S}}, \quad \tilde{S} = \sqrt{S_{ij}S_{ij}}, \quad S_{ij} = \frac{1}{2}\left(\frac{\partial u_j}{\partial x_i} + \frac{\partial u_i}{\partial x_j}\right) \tag{10}$$

The model constants are

$$C_{1\varepsilon} = 1.44, \quad C_2 = 1.9, \quad \sigma_k = 1.0, \quad \sigma_\varepsilon = 1.2 \tag{11}$$

The term G_k, representing the production of turbulence kinetic energy, is evaluated as:

$$G_k = \mu_t S^2 \tag{12}$$

where S is the modulus of the mean rate-of-strain tensor, defined as

$$S \equiv \sqrt{2S_{ij}S_{ij}} \tag{13}$$

For high-Mach-number flows, compressibility affects turbulence through the so-called "dilatation dissipation", which is normally neglected in the modeling of incompressible flows. Neglecting the dilatation dissipation fails to predict the observed decrease in spreading rate with increasing Mach number for compressible mixing and other free shear layers. To account for these effects in the k-ε models, the dilatation dissipation term, Y_M, is included in the k equation. This term is modeled as :

$$Y_M = 2\rho\varepsilon M_t^2 \tag{14}$$

where ($a = \sqrt{\gamma RT}$) is the speed of sound and M_t is the turbulent Mach No., defined as

$$M_t = \sqrt{2k/a^2} \tag{15}$$

Grid Mesh

The computations employ an unstructured, tetrahedral grid displaying 93845 nodes, 957859 faces and 462582 cells. Figure 3 displays a portion of the grid on train symmetry plane.

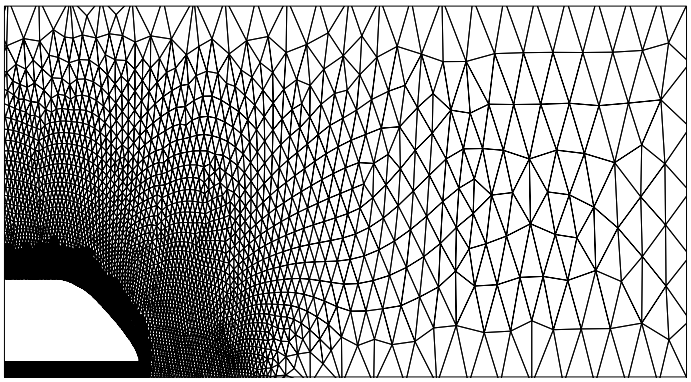

Figure 3. Half-sectional view of train symmetry plane grid

Boundary Conditions

The boundary conditions are specified on all boundaries of solution domain since the set of governing equations are Elliptic P.D.E.s. At the inlet boundary, the boundary values for the inlet flow velocity, inlet temperature, inlet turbulence intensity and length scale are specified. At the outlet boundary, the value of outlet pressure is specified; whereas gradient conditions are used for turbulence intensity, length scale and temperature.

Solid wall boundary conditions are used for the train body. Both fixed and moving wall boundary conditions are used for the computational domain bottom plane. Wall functions are used at all solid boundaries. The free stream velocity is taken to be 100 m/s to reflect the higher train speeds. The corresponding flow Reynolds number based on the train model height is 7.33×10^5 .

INVESTIGATIONS

In this section the results of the compressible flow computations for a stream velocity of 100 m/s are displayed and discussed. The computations are then repeated employing the incompressible assumption in order to assess compressibility effects. Furthermore, the computations are performed both with and without relative motion between ground and train.

Compressible Flow Over train without relative ground motion

Figures(4-9) display the results of the compressible flow calculations for flow over a train with a free stream velocity of 100 m/s(360 km/h), with a Mach number of about 0.294 based on mean train speed; which means that it can exceed 0.3 locally on some parts of the train surface. The velocity vectors represent in both magnitude and direction the local velocity.

Here X,Y and Z refer to display plane distances in the x,y, and z Cartesian coordinates directions, respectively; measured from an origin lying at the intersection of the bottom plane of the train, the train longitudinal symmetry plane, and the upstream plane of the trailing edge section. The x-direction is aligned with the longitudinal axis of the train(also free stream direction), the y-direction with the vertical, and the z-

direction with the horizontal lateral direction(also horizontal cross-stream direction). It is remarked that, for reasons of clarity, the coordinate scales in the horizontal and vertical directions are very different which causes the slender train body shape to appear bluff although it is not.

Figure 4 displays the velocity vectors over the train at the near edge longitudinal plane, Z=30 mm. It is clear that the flow is very smooth around the train body and that recirculation is absent, even at the trailing end.

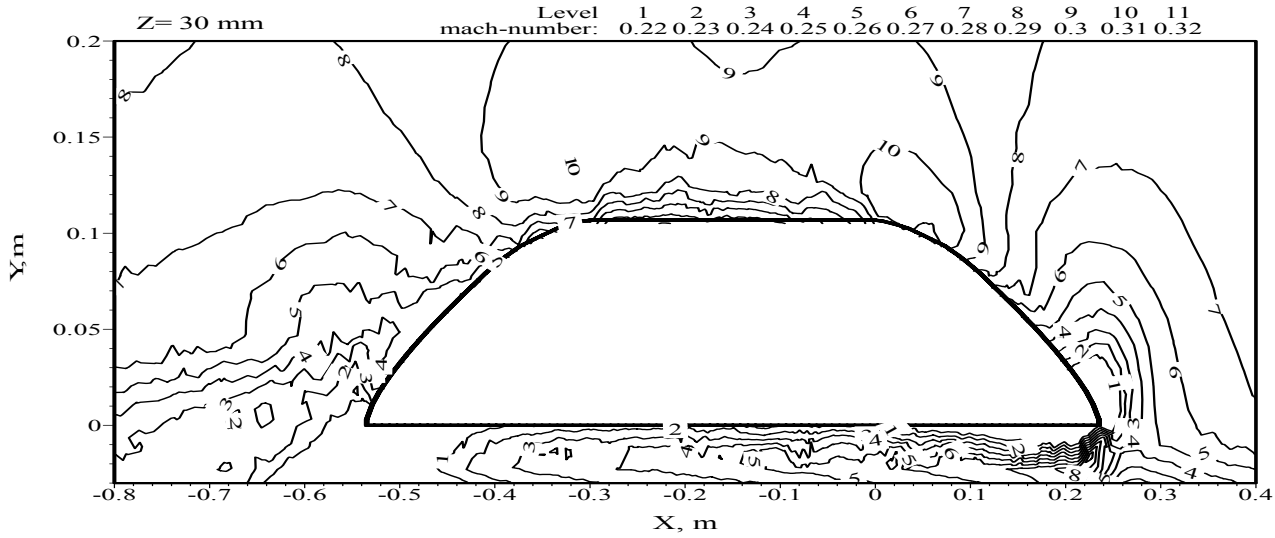

Figure 4. Velocity vectors at the longitudinal plane, Z=30 mm.

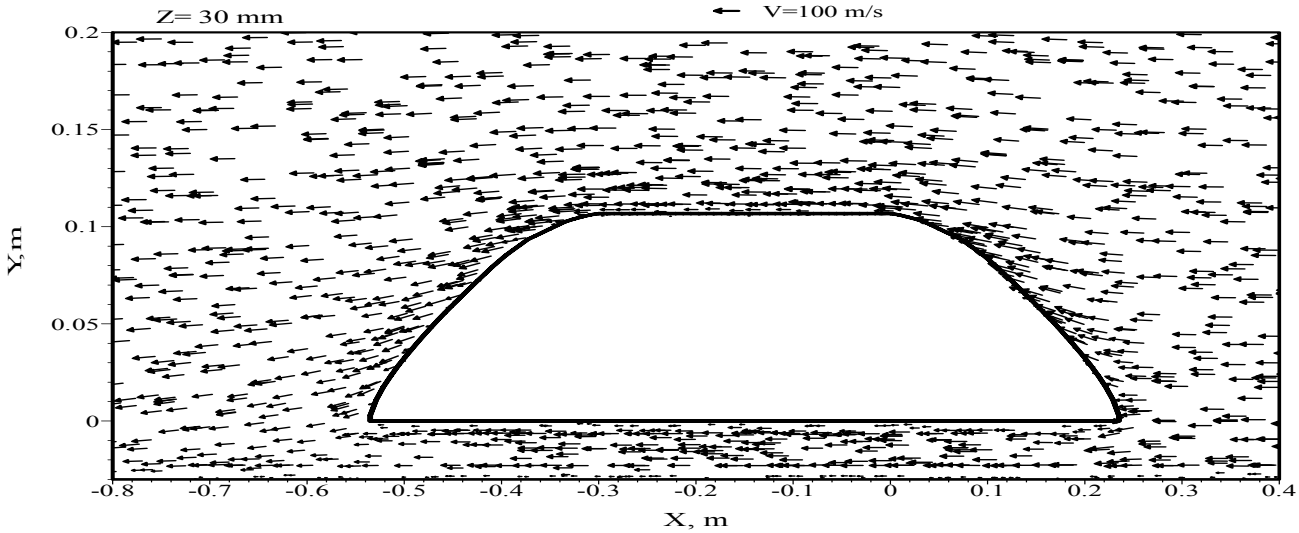

Figure 5. Mach number contour lines at Z=30 mm.

Figure 5 displays the corresponding Mach number contour lines. It is noticed that M values do not exceed 0.3 except in a small zone at the train front; and then barely so. Moreover, except for the region close to the ground, there is considerable symmetry of M contours at the front and rear ends, due to the symmetry of the geometry and absence of strong trailing edge recirculation.

Figure (6) shows the velocity vectors at the horizontal plane Y=40 mm, which lies at approximately 1/3 the way up the train. The flow is generally smooth, although there is an indication of a weak trailing edge vortex.

Figure (7) displays the corresponding M contours; it displays clear deviations between the contour lines at the leading and trailing ends, again confirming the presence of a trailing edge wake.

From both Figures(6,7) it is noticed that the flow is parallel over the main bulk of the train body, indicating that for the chosen train length/height ratio, the leading and trailing edge flows should not be affected by an increase of train length, thus justifying the reduction in the length/height ratio from that of real trains.

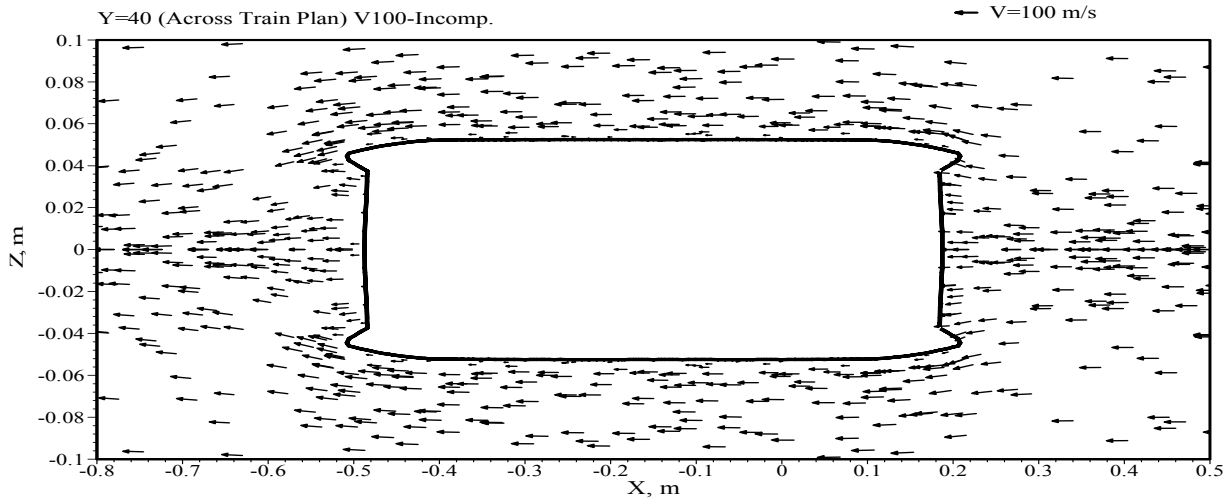

Figure 6. Velocity vectors in horizontal plane at Y=40 mm

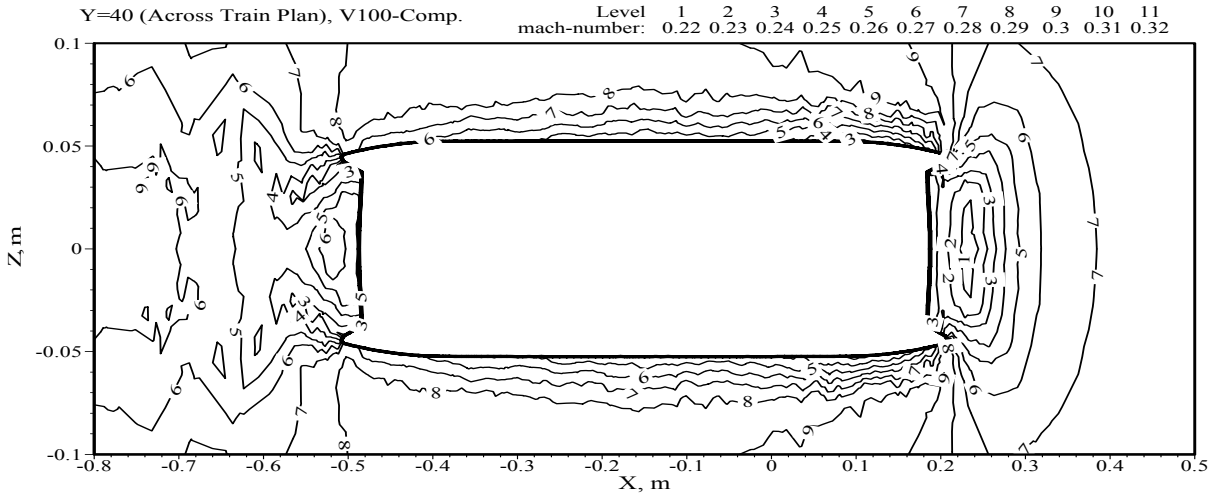

Figure 7. Mach number contour lines at Y= 40 m.m. plane.

Figure (8) displays the velocity vectors at three vertical cross-stream planes, located at the start of the trailing edge profile, approximately midway downstream, and at the trailing edge of the train. They reveal a secondary vortex on the two sides of the train and the formation of a fairly strong trailing edge vortex towards the rear. Figure (9) shows the corresponding Mach number distributions. Again the results indicate that the maximum M value is approximately 0.32 for those planes.

Assessment of Compressibility Effects

As revealed from the Mach number contours, no local spikes in value are present, and the maximum value of M is barely above that of the relative free stream velocity, and hardly above M=0.32. Comparison of the flow patterns, with and without compressibility introduced revealed very close agreement, Mohamed(2006). The comparison also indicated that compressibility causes density to increase in the leading edge by a maximum of only 3.2%, and to decrease in the

trailing edge by a maximum of 5.3%, relative to free stream density. Thus compressibility effects are minor for this type of flow. However, comparison of the predictions obtained at a train speed of 100 m/s, revealed a 10.7% decrease in the drag coefficient when compressibility effects are neglected.

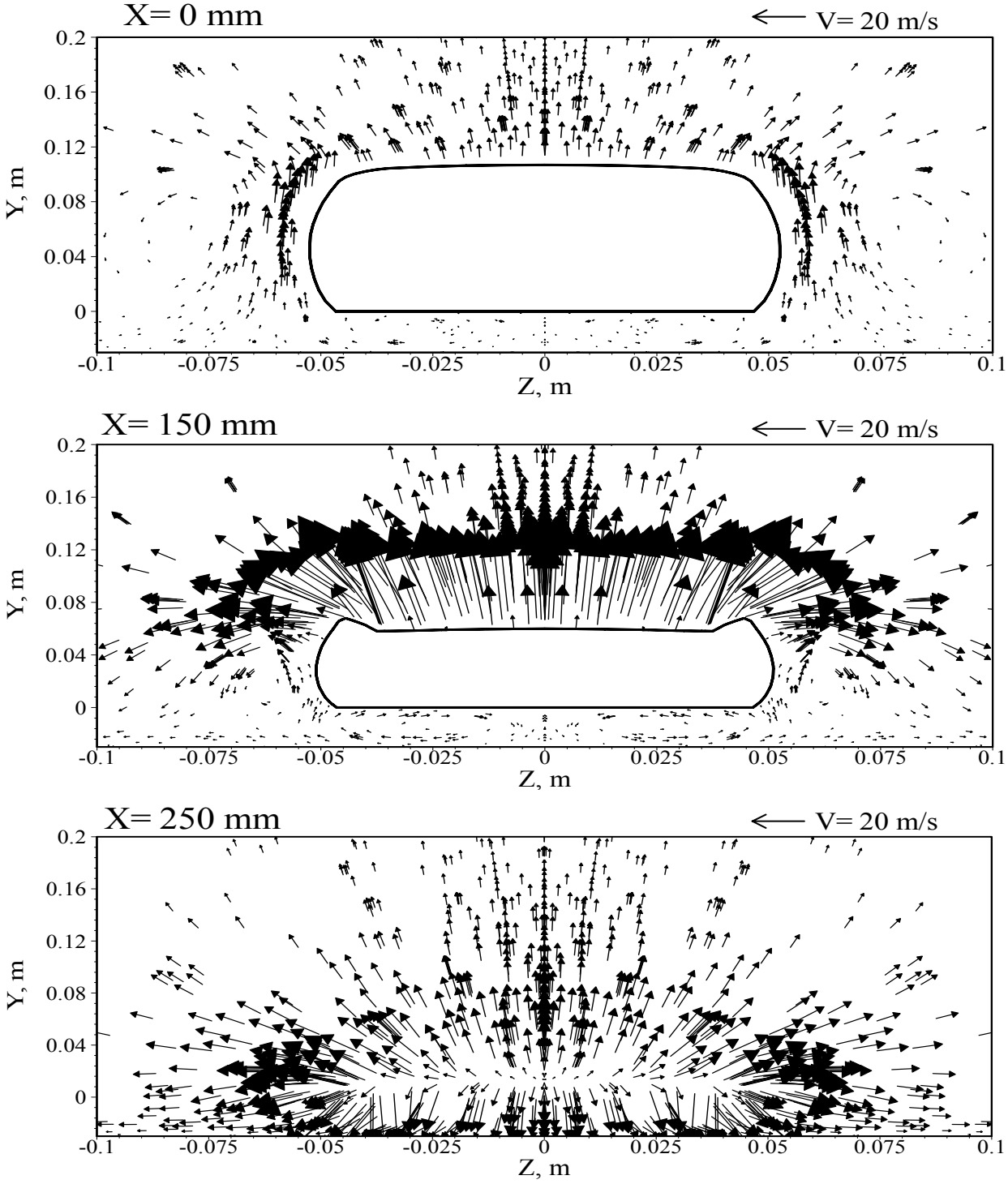

Figure 8.Velocity vectors at vertical cross-stream planes

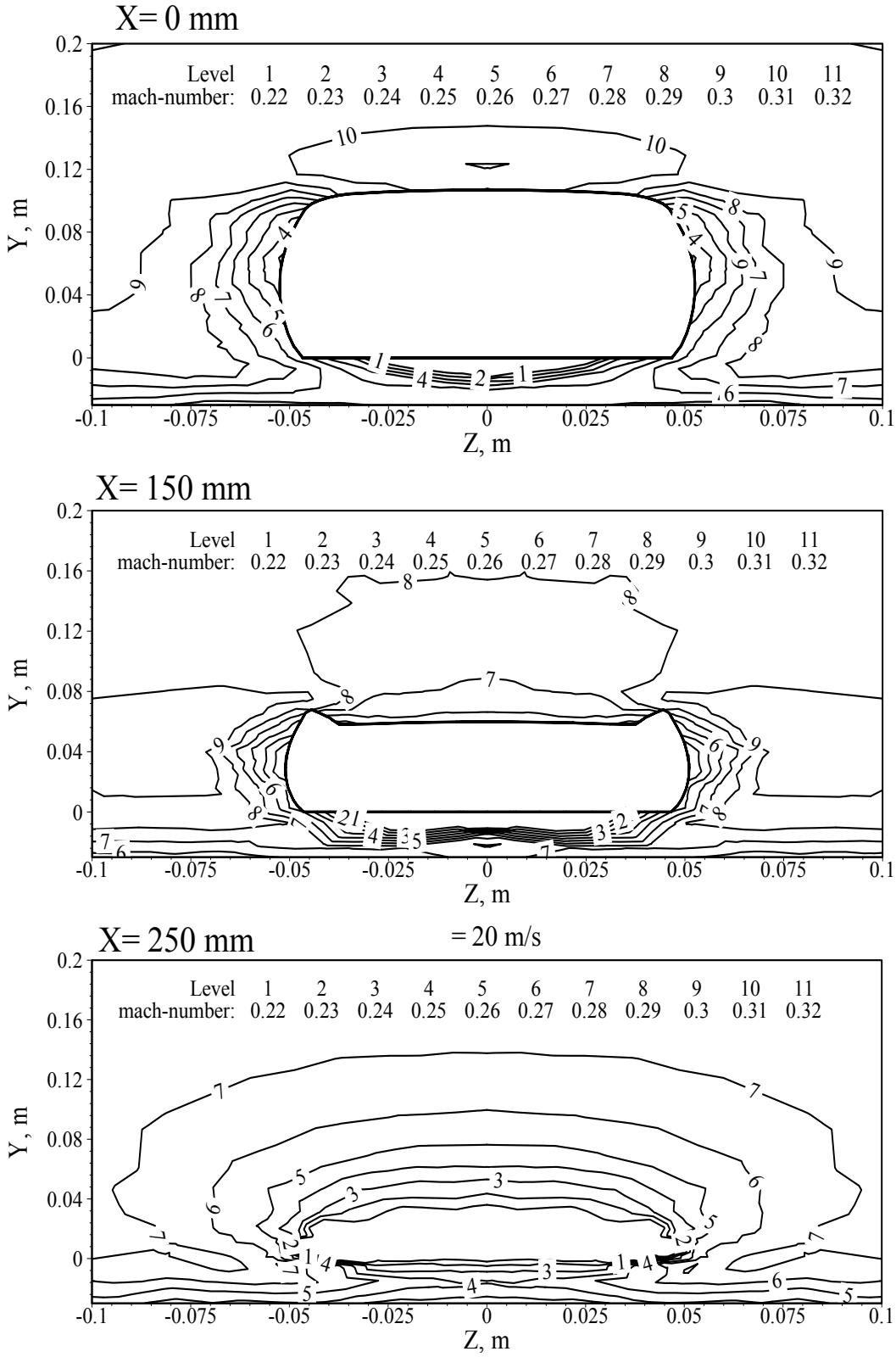

Figure 9. Mach number distribution at cross-stream planes

Assessment of Ground Effects

Most experimental investigations and many theoretical ones neglect the relative motion between the train and adjacent ground. An assessment is made here of the effect of neglecting this relative motion on the aero-dynamic drag forces. Thus similar computations were performed, with and without a moving ground relative to the train, and their results are compared.

Figure 10 displays the net sum of the train surface pressure forces, F_p, for various values of Reynold's number, Re, corresponding to different train speeds, i.e. the plot of the so called profile- or pressure-drag-force. Two plots are displayed together, the "FG" plot corresponding to fixed(stationary) ground relative to train, and the "MG" plot corresponding to moving ground relative to train. It is apparent that the ground effect is small, the pressure drag force being slightly higher when relative motion is not considered. This could be due to a steeper velocity gradient at the train bottom surface with fixed ground.

Figure11 displays the corresponding skin friction (viscous) drag forces, F_v; the same trend is revealed as for F_p. Figure 12 displays the corresponding plot for the total drag coefficients, C_d. The drag coefficient is seen to decrease slightly with Re, and to be over predicted when neglecting the relative motion of ground relative to train.

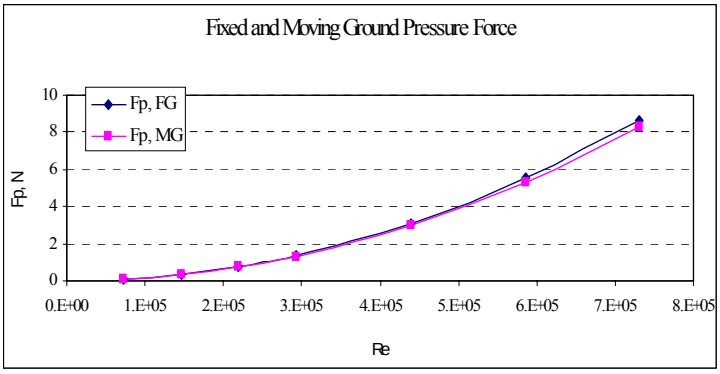

Figure 10. Profile Drag force for various train speeds

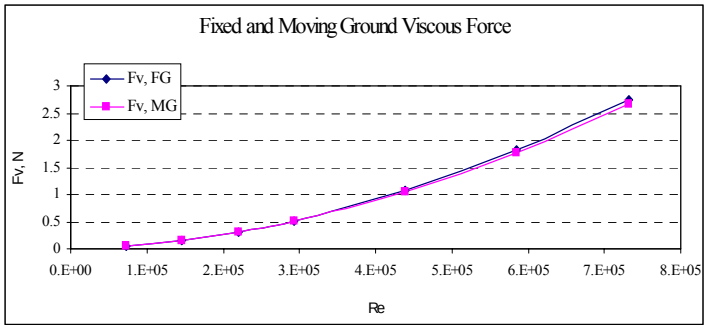

Figure 11. Skin friction Drag force for various train speeds

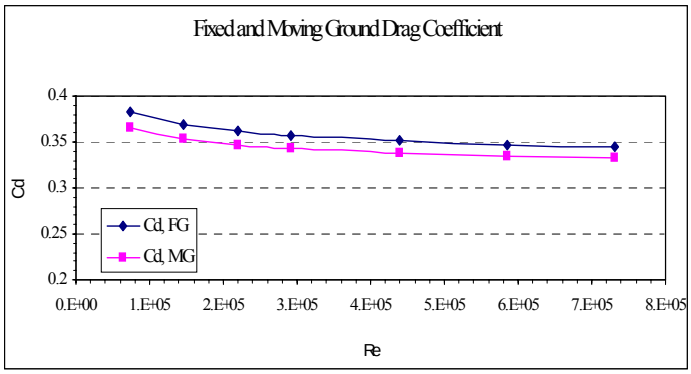

Figure 12 . Coefficient of Drag for various speeds

SUMMARY AND CONCLUSION

The paper presents the results of investigation of the flow over a new design for a high speed train, employing a mathematical model which adopts the RKE model of turbulence. The results of the investigations reveal that the new design, which features longitudinal nose/trailing end fins, displays much less trailing edge vortices, than conventional high speed train designs. This is reflected in a highly streamlined flow over the train body, and lack of large variations in Mach numbers.

The paper also assesses the effect of neglecting compressibility of the flow and relative motion between train and adjacent ground. Both effects are usually neglected in investigation of aerodynamics of trains; however, because the interest is in high speed trains it is important to assess the effect of this approximation on the accuracy of the results.

REFERENCES

Kohama Y., Fukunishi Y., Kobyashi R., Otaguro T., Ito J., Hattori M., Sato H., Matsui T., Okude M., Hayafuji H., and Takagi S., "Flow Measurement Around a High Speed Train", 5th Asian Congress of Fluid Mechanics, Aug. 10-14, 1992, Taejan, Korea.

King W.F. , Mackrodt P.A. and Pfizenmaier E. " The Aerodynamics and Acoustics of High-Speed Tracked Vehicles" Proc. Int. Conf. on Speedup Technology for Railway and Maglev Vehicles, B3-2-(3), Nov.22-26, 1993, Japan.

Raghu S.R., Kim H.D. and Setoguchi "Aerodynamics of High-Speed Railway Train" Progress in Aerospace Sciences, 38, 469-514, 2002.

Mohamed I.K., Experimental and Theoretical Investigation of the Flow Around High Speed Trains",PhD Thesis, Mechanical Engineering Department, Cairo University, 2006.

Shish, T.H. ,Liou,W.W., Shabbir,A.,Yang,Z. and Zhu,J. "A New k-ε Eddy Viscosity Model for High Reynolds Number Flows-Model Development and Validation" Computers Fluids,24(3):227-238,1995.